JEE Journal of Ecological Engineering

Journal of Ecological Engineering, 2026, 27(7), 86–98
https://doi.org/10.12911/22998993/218262
ISSN 2299–8993, License CC-BY 4.0

Received: 2026.02.03
Accepted: 2026.05.20
Published: 2026.06.01

From waste to bio-coal pathways: an integrated physicochemical and thermochemical characterization of food waste and cotton straw for hydrothermal carbonization

Islom Karimov[1*], Obid Tursunov [1,2], Nurislom Abduganiev[1], Bakhtiyor Meliyev[3], Shuhrat Turatov[4], Sitora Azimova[4], Kayum Karimov[5], Abdugani Rakhmatov[1], Irina Bozorova[5], Amangul Sanbetova[1]

[1] Department of Power Supply and Renewable Energy Sources, National Research University TIIAME, 100000 Tashkent, Uzbekistan
[2] College of Mechanical and Electrical Engineering, Shihezi University, Beisi Road, Shihezi, 832003 Xinjiang, China
[3] Department of Ecology and Labor Protection, Jizzakh Polytechnic Institute, 130100 Jizzakh, Uzbekistan
[4] Jizzakh Polytechnic Institute, Jizzakh 130100, Uzbekistan
[5] Department of Algorithms and Programming Technologies, Karshi State University, 180117 Karshi, Uzbekistan
* Corresponding author's e-mail: ikarimov.ilm@gmail.com

ABSTRACT

With increasing concerns about global climate change, along with other CO_2 mitigation measures, waste management is also being critical worldwide. On average, one-third of waste generated globally is food/organic waste, with high environmental hazards and low recycling rates globally. In this study, food waste and agricultural wastes were comprehensively studied in the perspective of solid fuel production by hydrothermal carbonization technology. This study investigates the suitability of food waste and cotton straw as feedstocks for hydrothermal carbonization aimed at producing high-quality solid bio-fuel. Municipal solid waste characterization in Tashkent revealed that food waste consistently represents the largest fraction of household waste (47–52 wt%), with total biodegradable organics exceeding 54 wt%, confirming its steady availability for thermochemical valorization. Structural carbohydrate analysis showed that food waste is rich in cellulose (45.22 ± 2.1%), hemicellulose (29.39 ± 1.8%), and lignin (25.47 ± 1.5%), forming a balanced lignocellulosic matrix favorable for hydrothermal carbonization reactions. Proximate analysis demonstrated significantly higher volatile matter (77.79 wt%) and lower ash (6.97 wt%) in food waste compared to cotton straw, alongside an High Heating Value of 23.18 MJ/kg, indicating strong potential for generating energy-dense hydrochar comparable to sub-bituminous coal. Food waste demonstrated superior characteristics for hydrothermal carbonization compared to cotton straw, with 34% higher volatile matter and 70% lower ash content. Thermogravimetric analysis revealed a multistage decomposition pattern involving moisture evaporation, primary and secondary pyrolysis, and high-temperature gasification, with activation energy trends consistent with the sequential degradation of hemicellulose, cellulose, and lignin. Kinetic analysis revealed lower activation energy for FW pyrolysis (50.7 kJ/mol primary stage) versus cotton straw (122 kJ/mol), suggesting more favourable conversion energetics. FTIR analysis of both food waste and cotton straw confirmed dominant oxygenated functional groups (O–H, C–H, C=O, and C–O), supporting the expected hydrothermal carbonization pathways of dehydration, decarboxylation, and aromatization that contribute to carbon densification. Overall, the integrated physicochemical, thermal, and spectroscopic characterization establishes FW as a highly suitable and abundant feedstock for hydrothermal carbonization-based bio-coal production, either as a standalone substrate or as a co-feed with agricultural residues such as cotton straw.

Keywords: hydrothermal carbonization, FW valorization, agricultural residue, hydrochar/bio-coal, thermochemical characterization, waste-to-energy.

INTRODUCTION

Uzbekistan, with a population exceeding 33 million, generates significantly higher amounts of municipal solid waste (MSW) than other Central Asian countries, reaching about 35 million m³ annually, while more than 100 million tons of industrial and municipal waste are disposed of in landfills each year, accumulating over 2 billion tons to date (Tursunov et al., 2023). In Tashkent city alone, daily waste generation has ranged from 1500 to 2100 tons between 2020 and 2024, exerting considerable pressure on major landfill sites such as Okhangaron and Tulabek (Tursunov et al., 2024). Rapid urbanization, lifestyle changes, and rural-to-urban migration further intensify the burden on existing disposal infrastructure, highlighting the urgent need for sustainable waste valorization pathways. Given that a substantial share of household solid waste in developing countries is organic in nature (Sharma et al., 2020; Tursunov et al., 2023), the conversion of FW and abundant agricultural residues such as CS into value-added bio-coal via HTC represents a promising local strategy (Tursunov et al., 2023).

Globally, MSW generation reached approximately 2.01 billion tons in 2016 and is projected to increase to 3.4 billion tons by 2050, driven by population growth, rapid urbanization, industrialization, and changing consumption patterns (Tursunov et al., 2023), (Tursunov et al., 2025). About one-third of global waste is still disposed of in open dumps, particularly in developing countries, while recycling rates remain as low as 5%, leading to severe environmental and public health consequences. The high organic fraction of MSW—often exceeding 50% in developing regions—results in the emission of hazardous gases such as CH_4, CO_2, H_2S, and NH_3 from landfills (Sharma et al., 2020a), contributing to climate change and ecosystem degradation (Tursunov et al., 2025). The sustained growth of the global population and continuous industrial expansion drive an escalating demand for energy, prompting an intensive search for sustainable energy alternatives (Kang et al., 2019). Simultaneously, the world confronts a profound challenge in managing the enormous volumes of organic waste generated annually (Sharma et al., 2020). FW, a significant fraction of MSW, and abundant agricultural residues represent highly challenging feedstocks for conversion due to their high moisture content, which can typically range from 70% to 90% in unprocessed streams (Pecchi et al., 2020; Yusuf et al., 2020). This high-water content renders conventional thermal conversion methods (such as pyrolysis or incineration) inefficient, demanding an energy-intensive and costly pre-drying step (Babinszki et al., 2020; Sharma et al., 2020). While alternative recycling methods like composting and anaerobic digestion are practiced, they are often constrained by long reaction times and the biological instability of FW. Therefore, developing effective, low-energy solutions for upgrading these wet organic resources into stable, energy-dense products is a global necessity.

HTC has emerged as a promising technology perfectly suited to bypass the critical obstacle of high moisture content (Antero et al., 2020; Xu et al., 2020; Yusuf et al., 2020). HTC is a wet thermochemical conversion process that simulates natural coalification, typically operating at mild subcritical water conditions, generally between 180 and 350 °C and under autogenous pressure (Khan et al., 2019; Yusuf et al., 2020). The core technical advantage of HTC lies in its use of water as the reaction medium; at elevated temperatures, water acts as a reactive, non-polar solvent and catalyst, facilitating crucial chemical transformations without prior drying (Krysanova et al., 2019; Wüst et al., 2019; Mazumder et al., 2022; Reza et al., 2014). The fundamental reaction mechanisms include a complex network of ionic pathways such as hydrolysis, dehydration, decarboxylation, polymerization, and aromatization (Babinszki et al., 2020; Sharma et al., 2020;). These reactions result in the breaking of complex polymeric bonds (cellulose and hemicellulose degrade readily at temperatures as low as 180–230 °C) and a reduction in the oxygen-to-carbon (O/C) and hydrogen-to-carbon (H/C) atomic ratios, a process that concentrates carbon and upgrades the fuel quality (Xu et al., 2020; Sharma et al., 2020; Reza et al., 2014).

HTC is versatile, accepting a wide spectrum of feedstocks, including lignocellulosic biomass (LCB) such as agricultural residues (e.g., miscanthus, corn stalk, wheat straw, olive pulp) and aquatic plants (e.g., *Azolla*), alongside urban wastes like FW (FW) and sewage sludge (SS) (Khan et al., 2019). FW is particularly relevant due to its volume and high content of easily hydrolyzed carbohydrates and proteins (Wang et al., 2020). For FW and LCB, HTC produces an energy-dense solid product known as hydrochar or bio-coal, typically exhibiting fuel properties

comparable to lignite. The HHV of FW can be increased significantly, rising from initial values (e.g., 25.1 MJ/kg) to over 33.1 MJ/kg. This increase is attributed to the removal of low-energy oxygen and hydrogen atoms. Critically, the HTC process dramatically reduces the ash and alkali metal content (specifically K and Na) by dissolving these inorganics into the process liquid. This demineralization significantly mitigates the risk of fouling and slagging during subsequent combustion, a major advantage over traditional dry carbonization methods (Gao et al., 2019).

Furthermore, co-HTC(co-HTC), which involves treating FW or Ag waste alongside low-quality materials such as coal waste (CW) or sewage sludge (SS), provides synergistic benefits (Mazumder et al., 2022). The organic acids formed during the HTC of FW (like formic and acetic acid) create a mildly acidic environment that actively aids the leaching of undesirable inorganic elements, such as ash and sulfur, from the blended material (Saba et al., 2017). For instance, co-HTC of CW and FW has been shown to reduce sulfur content from 9.6% in raw CW to 2.1% in the resultant hydrochar, while increasing its elemental carbon content (Mazumder et al., 2022). This demonstrates the power of co-HTC in converting heterogeneous, challenging wastes into high-quality, homogenized solid fuels suitable for applications such as co-firing in existing coal power plants. The physical properties of hydrochar are also improved, becoming highly hydrophobic and friable, enhancing durability for storage and reducing transport costs by increasing energy density. These hydrochars also display higher thermal stability and increased ignition temperatures compared to raw biomass, reducing the risk of spontaneous combustion during storage.

To comprehensively assess the production of these clean solid fuels, a rigorous list of tests and laboratory analyses is required for both the feedstock and the resultant hydro char.

Compositional and energetic analysis: Includes proximate analysis (volatile matter, fixed carbon, ash content) and ultimate analysis (C, H, N, S, O content), crucial for determining fuel quality indicators like the H/C and O/C ratios (Gao et al., 2019). The HHV is essential for quantifying energy density and is determined via bomb calorimetry (Wilk et al., 2021).

Thermal stability and combustion performance: TGA and derivative thermogravimetric analysis (DTG) are necessary to study thermal decomposition profiles, kinetic parameters (e.g., activation energy, determined using methods like the Kissinger-Akahira-Sunose (KAS) or FWO methods (Krysanova et al., 2019; Wilk et al., 2021), ignition temperature T_i, and burnout temperature T_b to evaluate combustion reactivity (Saba et al., 2017).

Structural and chemical characterization: FTIR spectroscopy identifies functional groups (e.g., hydroxyl, carbonyl). SEM and potentially XPS and N2 adsorption (BET method) detail the morphological features, porosity, surface area, and confirm the degree of carbonization (Fu et al., 2019).

Inorganic and process liquid analysis: ICP or XRF analyses track metal migration (e.g., alkali metals, heavy metals) and quantify critical nutrients (N, P) in both solid hydro char and the aqueous co-product (Krysanova et al., 2019). Process water requires analysis for its COD and TOC to evaluate its environmental and energetic reuse potential (Gao et al., 2019). The effective management of the liquid co-product is paramount for the overall economic viability of the HTC process, as this stream contains a high concentration of dissolved organics and leached nutrients (Wüst et al., 2019). This liquid phase can be recirculated back into the HTC process or directed toward anaerobic digestion (AD) for enhanced biogas (methane) production, thus potentially achieving a self-sustaining, negative energy output solution for municipal and agricultural waste valorization (Gao et al., 2019).

While numerous studies have investigated HTC of individual biomass types, comparative analyses of contrasting urban and agricultural waste streams within specific geographic contexts remain limited. Moreover, integrated characterization linking compositional properties to thermal kinetics and chemical functionality provides more predictive power for HTC optimization than isolated analyses. This study addresses these gaps through systematic comparison of FW (heterogeneous urban stream) and CS (homogeneous agricultural residue) prevalent in Uzbekistan. Specifically, we aim to: (1) quantify and compare compositional characteristics relevant to HTC, (2) elucidate thermal decomposition kinetics and energetics, (3) identify key functional groups influencing HTC pathways, and (4) establish criteria for feedstock selection and blending strategies for optimized bio-coal production.

This study aims to thoroughly investigate physical-chemical properties of municipal and agricultural waste samples, for the purpose of further

applying them to HTC technology. A rigorous assessment of HTC technology will be conducted for converting widespread food and agricultural wastes into sustainable solid fuels, detailing the process parameters required to maximize fuel quality while minimizing environmental impact.

METHODS

Sampling and sorting procedures

Waste composition is described as the characterization of solid waste represented by a breakdown of mixture into specified waste components on the basis of mass fraction or of weight percent (ASTM, 2016). To investigate waste types and their share in MSW, a compositional study was carried out in 2 different districts in Tashkent city. The studies were done on autumn and summer seasons. Two random WCP were chosen for gathering waste samples. As per American Society for Testing and Materials (ASTM) D 5231-92 standard, sorting sample weight is required to be 91–136 kg in order to represent the characteristics of a vehicle load of MSW (ASTM, 2016). Thus, in this study, a 100 kg waste samples were extracted from WCP. The samples were taken from the bins to the special bags and weighted by a scale.

A clean, flat area was prepared as required on ASTM procedure, and waste bags were unpacked. Normally, each portion of MSW is placed in a separate plastic bag and there are plenty of them. Thus, waste needs to be unpacked from plastic bags to form representative sample. Then, unpacked waste pile was thoroughly mixed from four sided by a shovel. Following that, by using quartering method, well mixed waste pile was divided into four equal parts and two diagonal sides were discarded. The other two sites were taken as a representative sample of a MSW for sorting stage. In the sorting stage, samples were mixed second time by a shovel and the segregation process was done. Based on ASTM D 5231-92 waste composition data sheet, seven main types of waste were sorted, namely: paper, plastic, food waste, ferrous, glass, textile and others (ASTM, 2016). First, all the plastics were sorted as they abundant among waste mixture. Then, paper, textile, glass and metals were collected respectively. On the final stage, FW and other types were separated. Sorted waste fractions were put in seven labelled special plastic bags and the weight of each fraction were identified by a scale. In the end, results were recorded to the waste composition data sheet. For further laboratory analyses, a kilo of sample from each fraction was taken.

Sample preparation for laboratory analyses

FW and CS samples were collected from local sources in Tashkent city in Uzbekistan, and prepared for subsequent analyses. FW samples underwent pre-weighing using calibrated electronic scales to ensure accuracy, followed by drying in an electric thermostatic blast drying oven (model: GZX – 9140 MBE) at 105 °C for 4 hours to remove residual moisture, resulting in approximately 10.3% moisture content. The samples were cooled at room temperature and re-weighed to determine final dry mass. CS samples were first cut into 5-8 cm pieces to ease further size reduction processes, and then dried overnight in a blast drying oven (model: LC-101-2B) at 65 °C.

Both FW and CS dried samples were ground using high-speed universal grinders (model: FW-100 and 2000c) to achieve fine particle sizes. Ground materials were then sieved using a vibratory sieve shaker (model: Retsch AS 200) equipped with 1 mm and 0.15 mm meshes to separate particles into three size fractions: less than 1mm, 0.15 to 1 mm, and higher than 0.15 mm as per other research works (Periyavaram et al., 2023; Wu et al., 2023; Yan et al., 2023). Sieved fractions were packaged in labelled plastic containers for further laboratory analyses.

Proximate, ultimate and chemical analysis

Table 1 shows the summary of the proximate analysis protocol applied to FW and CS samples. As described above, moisture content was determined by weight loss of the original wet sample after oven-drying until constant mass is achieved, and calculated according to ASTM D-3173. Volatile matter was determined by heating 1.0 ± 0.1 g of sample in a crucible inside a muffle furnace (model SX2-5-13E) at 950 °C for 7 min following ASTM D3175. Ash content was measured by complete combustion of 1.0 ± 0.1 g of sample in a crucible at 750 °C for 4 h according to ASTM D3174. Fixed carbon was calculated by difference using the standard equation given in Table 1.

To determine the elemental of food waste and cotton straw, an ultimate analysis was conducted using Eltra CHS-580 and German Element

Table 1. Procedure of conducting proximate analysis

Samples	Process	Equipment/Device used	Process settings/conditions	Formula
FW	Moisture content	GZX – 9140 MBE	105 °C for 4 hours	
CS		LC-101-2B	65 °C overnight	
FW	Volatile matter	Muffle Furnace SX2-5-13E	950°C for 7 minutes (based on ASTM D3175)	$\%\mathrm{VM} = \frac{(W_{sample} - W_{ash})}{W_{sample}}$
CS				
FW	Ash content		750°C for 4 hours (based on ASTM D3174)	$\%\mathrm{Ash} = \frac{(W_{sample} - W_{ash})}{W_{sample}} \times 100$
CS				
FW	Fixed carbon	By calculation	$\%FC = 100(\%moisture + \%volatile\ matter + \%ash)$	
CS				

Analyzers (Model: UNICUBE) analyzer. The cellulose, hemicellulose, and lignin percentages in CS raw materials were measured using the Van Soest Method of Detergent Fiber Analysis (Elshareef et al., 2025).

TGA and HHV analyses

TGA was conducted to evaluate the thermal decomposition behavior and stability of FW and CS samples, which was considered as a feedstock for HTC. The analysis was performed using a thermogravimetric analyzer (model: TGA 5500, TA Instruments, USA) under a controlled atmosphere. A sample mass of approximately 6.5 mg was weighed and placed in an alumina crucible. The analysis was carried out under a constant flow of helium gas (25 mL/min) to maintain an inert atmosphere and prevent oxidation. The sample was heated from temperature 30 °C up to a final temperature 900 °C at a constant heating rate of 10 °C/min. The continuous change in sample mass and the corresponding temperature was recorded. The derivative thermogravimetric (DTG) curves, representing the rate of mass loss were calculated from the raw TGA data. The TRIOS program was used to analyze the recorded data

Higher heating value (HHV) and lower heating value (LHV) of FW and CS were identified by IKA C5000 bomb calorimeter, and an average result of triplicate measurements were taken as a final result.

FTIR analysis

Fourier-transform infrared spectroscopy (FTIR) analysis was performed to identify the functional groups present in FW and CS samples. The analysis was conducted in the laboratory of the College of Mechanical and Electrical Engineering at Shihezi University. M-FTIR was employed for sample analysis (model: Nicolet iN10, thermo scientific). The raw FW and CS samples were dried and ground prior to analysis to ensure homogeneity and proper signal acquisition. The recommended sample size for reliable spectral acquisition was between 0.1 to 1 mm. While the lower analytical limit of the instrument was 0.1 mm, this specific range was targeted during sample preparation to optimize the signal-to-noise ratio and reproducibility. The spectra were recorded over a range of 4000–400 cm^{-1} wavenumbers with a specific resolution and 16 scans to ensure high-quality data. Background scans were taken before each sample measurement and subtracted from the sample spectra. The resulting spectra were analyzed to identify characteristic peaks corresponding to different functional groups, providing insight into the chemical changes.

RESULTS

Municipal solid waste composition

Figure 1 (a, b) shows the composition of MSW collected from 2 different districts in order to increase reliability of data. From Figure 1a, FW dominates the waste stream at 52 wt%, followed by bones (13 wt%) and minor fractions of paper, textiles, diapers, metals, glasses, and others. This high organic content (approximately 66 wt% combined FW and bones) makes the waste highly suitable as feedstock for HTC to produce bio-coal.

While on Figure 1b, FW remains the largest fraction at 44 wt%, with significant contributions from plastics and glasses (13 wt% each), bones (6 wt%), and paper/textiles (7 wt% each). The total biodegradable organic fraction (FW + bones +

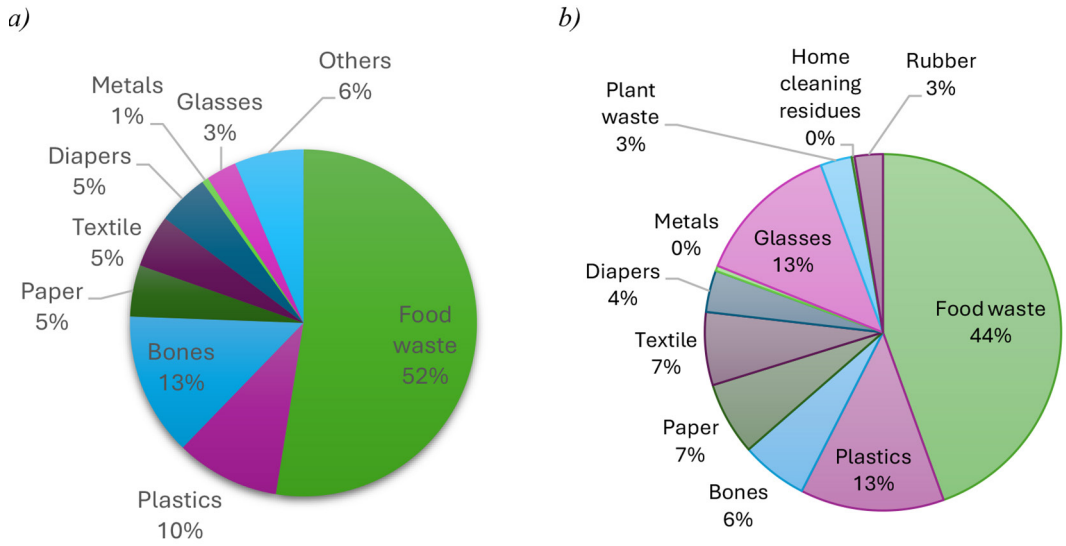

Figure 1. Morphology of municipal waste collected from (a) Chilanzar and (b) Mirzo Ulugbek districts

plant waste) exceeds 54 wt%, confirming strong potential for HTC-based valorization across different districts of Tashkent city in Uzbekistan, despite noticeable variations in recyclable contents (plastics, glass, and metals).

Figure 1a, 1b demonstrates that FW constitutes 44–52 wt% of MSW in Tashkent city, providing a consistent and abundant lignocellulosic-rich feedstock for HTC processes aimed at sustainable bio-coal production.

Chemical composition, proximate, ultimate and HHV analyses

Structural carbohydrates in biomass sample

Table 2 presents the average lignocellulosic composition of the FW and CS samples used in this study, determined through standard chemical fractionation methods. The results reveal that FW is predominantly carbohydrate-rich, with cellulose constituting 45.22 wt%, hemicellulose 29.39 wt%, and lignin 25.47 wt% on a dry-weight basis (values represent the mean of triplicate analyses). The three major polymeric fractions sum to 100 %, confirming complete recovery and the absence of significant extractives or ash interference in the analyzed samples after pre-treatment. This relatively balanced distribution – higher cellulose and hemicellulose content compared to typical woody or herbaceous biomass – highlights the favorable suitability of FW as a feedstock for biochemical and thermochemical conversion processes targeting value-added energy products, such as bio-coal. The chemical composition of CS is dominated by cellulose (42.50 wt%), followed by hemicellulose (17.32 wt%) and lignin (15.11 wt%), confirming its typical lignocellulosic biomass nature. The relatively high cellulose content suggests a strong contribution to volatile release during primary pyrolysis, as cellulose decomposes rapidly in the temperature range of 300–370 °C (Elshareef et al., 2025).

Proximate and ultimate analyses of biomass samples

Table 2 shows the proximate analysis of the two HTC feedstocks. FW exhibits 59.46 wt% volatile matter, 22.65 wt% ash, and 4.61 wt% fixed carbon. In contrast, CS contains 74.03 wt% volatile matter, 0.70 wt% ash, and 21.7 wt% fixed carbon. Therefore, FW is characterized by significantly higher ash and lower fixed carbon content compared to CS. The high volatile matter indicates good reactivity and suitability for thermochemical conversion, while the relatively high fixed carbon fraction reflects the contribution of lignocellulosic structures to char formation. The exceptionally low ash content is a significant advantage, as it minimizes slagging, fouling, and inorganic accumulation during HTC or combustion. It makes CS particularly suitable as a structural biomass feedstock or as a co-feedstock to dilute ash-rich materials in blended HTC systems.

The ultimate analysis of FW reveals a lower carbon content (25.81 wt%) compared to CS, but substantially higher hydrogen (16.02 wt%) and oxygen (55.93 wt%) contents. This composition

Table 2. Proximate, ultimate, HHV and chemical compositions of FW and CS samples

Sample	Food waste	Cotton straw (Elshareef et al., 2025)
Proximate analysis (%)		
Moisture content	10.28	3.57
Volatile matter	59.46	74.03
Ash content	22.65	0.70
Fixed carbon	4.61	21.7
Ultimate analysis (%)		
Carbon	25.81	44.41
Hydrogen	16.02	5.4
Nitrogen	2.02	1.11
Sulphur	0.19	0.23
Oxygen (by difference)	55.93	48.85
High Heating Value (MJ/kg)	23.18	16.55
Chemical composition		
Cellulose	45.22	42.50
Hemicellulose	29.39	17.32
Lignin	25.47	15.11

Note: all samples were used on dry basis.

reflects the dominance of lipids, proteins, and carbohydrates typically present in food residues. The elevated hydrogen content contributes positively to the high HHV (23.18 MJ/kg), while the higher nitrogen content (2.02 wt%) indicates the presence of proteinaceous matter, which may lead to increased nitrogen-containing gaseous emissions during thermochemical processing. Despite the lower carbon fraction, the ultimate analysis confirms that FW possesses high intrinsic energy potential, making it a highly attractive feedstock for HTC, especially when combined with lignocellulosic materials to balance elemental composition.

The ultimate analysis shows that CS contains a high carbon content (44.41 wt%) and oxygen content (48.85 wt%), with comparatively low hydrogen (5.40 wt%) and nitrogen (1.11 wt%) contents. The elevated carbon fraction is beneficial for solid fuel applications, as it directly contributes to energy density. However, the high oxygen content reflects a lower degree of natural carbonization, which explains the relatively modest heating value of the raw material (Borges et al., 2026). The low nitrogen and sulfur contents are environmentally favorable, as they imply reduced NO_x and SO_x emissions during thermochemical conversion. Overall, the ultimate analysis suggests that CS is a clean but oxygen-rich feedstock, requiring upgrading (e.g., HTC) to enhance carbon concentration and fuel quality.

Higher heating values

The HHV of 23.18 MJ/kg is comparable to that of sub-bituminous coal and significantly higher than many lignocellulosic biomasses, confirming the excellent energetic potential of FW-derived hydro-char after HTC upgrading. CS exhibits an HHV of 16.55 MJ/kg, which is typical for untreated agricultural residues and notably lower than that of FW. This lower HHV is primarily attributed to the high oxygen content and limited lignin fraction, which reduce intrinsic energy density. Nevertheless, the HHV remains within the range suitable for bioenergy applications, and significant enhancement is expected after HTC due to dehydration, decarboxylation, and carbon enrichment. Therefore, CS represents a promising precursor for solid biofuel upgrading, particularly when HTC severity is optimized or when co-processed with high-energy feedstocks.

Blending high-volatile, low-ash FW with CS in HTC can yield hydro-char with optimized volatile/fixed-carbon ratios, reduced ash-related slagging risks, and calorific values suitable for solid biofuel applications.

Thermogravimetric analysis of biomass samples

Figure 2 (a and b) shows TGA and DTG test of biomass sample which explain four stages

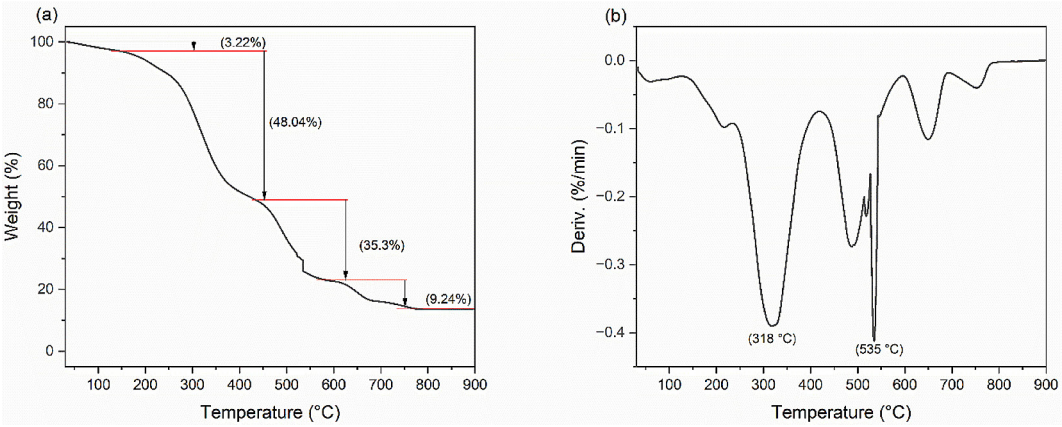

Figure 2. TGA (a) and DTG (b) graphs of FW sample

indicating moisture content evaporation, primary pyrolysis, secondary pyrolysis, and gasification. The first stage represents moisture evaporation occurred between 30 and 140 °C with moisture loss of 3.22%. The second and third stages (primary and secondary pyrolysis) demonstrated maximum weight loss occurred between 140 and 590 °C with weight loss of 48.04 and 35.3% showing significant peaks of 318 and 535 °C on DTG curve respectively. Due to decomposition of cellulose and hemicellulose, the final stage of biomass sample degradation (gasification) started after 590 °C and followed by a linear pattern when the temperature attained 770°C, where lignin content will be decomposed in this stage to form ash and biochar products (Elkhalifa et al., 2025). Studies have revealed that the thermal degradation stages of biomass could be categorized as water evaporation, volatile matter release, and gradual carbonization of solid materials (Indira and Parameswaran, 1986; Zhou et al., 2006).

Based on the TGA curves, it can be concluded that after evaporation of physically adsorbed water and light volatiles, the tested waste undergoes a basic thermal decomposition, in which primary pyrolysis (from 140 to 430 °C) and subsequent secondary pyrolysis (up to 590 °C) can be distinguished. Biomass pyrolysis is normally explained by the decomposition of its main components i.e. cellulose, hemicellulose, and lignin. Indeed, there are no certain temperature ranges stated for their decomposition, but it is believed that hemicellulose and cellulose decomposition is in the ranges of 200–350 °C and 240– 500 °C. In turn, the decomposition rate of lignin is quite slower, even covering a wider temperature range of 150–900 °C (Ganeshan et al., 2018); (Özsin and Pütün, 2017). Therefore, it can be assumed that primary pyrolysis is related to the collective contribution from hemicellulose and extractives (e.g. proteins, starches, lipids, and sugars) (Liu et al., 2020). In turn, secondary pyrolysis is associated with cellulose decomposition, whereas small sections of both pyrolysis are associated with the decomposition of lignin (Elkhalifa et al., 2025). Finally, the TGA curve shows another slight mass change above 590 °C, which is probably associated with the decomposition of carbonaceous materials retained in the residue and/or decomposition of calcium carbonate generated from the decomposition of organic calcium compounds in the analysed FW sample (Liu et al., 2020).

The Coast and Redfern method was chosen to calculate the kinetic parameters of the thermal decomposition of FW (Table 3), and this choice is justified in the literature (Elkhalifa et al., 2025; Indira and Parameswaran, 1986; Zhou et al., 2006; Ganeshan et al., 2018).

The parameters listed in Table 3 indicate that pyrolysis of FW comprises a multistage reaction in which each single reaction contributes partially to the whole mechanism at different extents. Nevertheless, the high values of R^2 (above 0.9700) were recorded for both pyrolysis, thus it can be assumed that the model used reflects very well the measurements data. The low value of E_a for primary pyrolysis results from the degradation of unstable hemicellulose and extractives with small molecules (Xu and Chen, 2013). In turn, the E_a value for secondary pyrolysis is more than 4 times higher, which is influenced by the fact that the more stable cellulose is decomposed here. Moreover, it is possible that minerals in food samples hindered the diffusion of heat and the release of degraded volatiles during secondary pyrolysis

Table 3. Kinetics parameters of FW pyrolysis

Stage	E_a (kJ/mol)	A (1/min)	n (-)	R^2 (-)
Primary pyrolysis	50.7	1.54E+03	1.22	0.9705
Secondary pyrolysis	234.5	8.13E+14	1.68	0.9716

(Liu et al., 2020), which also affected the value of activation energy. Finally, a high value of the pre-exponential factor *A* during secondary pyrolysis indicates a slow and hard degradation effect (therefore, a high rate of molecular collisions, i.e., high reaction energy, was needed) (Liu et al., 2020). Comparable values of E_a for biomass pyrolysis can be found in the literature (Elkhalifa et al., 2025; Ganeshan et al., 2018; Özsin and Pütün, 2017; Liu et al., 2020). As for the reaction order *n*, a slightly higher one was obtained for the secondary pyrolysis, however similar values of *n*, i.e. between 1–2 can be found in the literature (Ganeshan et al., 2018).

The thermogravimetric (TG) and derivative thermogravimetric (DTG) profiles of CS indicate (Figure 3) a three-stage thermal decomposition behavior, characteristic of lignocellulosic biomass. In the first stage, occurring between 30 and 200 °C, a minor weight loss of approximately 2.7% is observed, which is attributed to the evaporation of physically bound moisture and light volatiles. The low mass loss in this region confirms the relatively low inherent moisture content of the material. This stage is thermally mild and does not involve significant structural decomposition of the biomass components.

The second stage, corresponding to primary pyrolysis, takes place over the temperature range of 200–370 °C and represents the most significant mass loss, accounting for approximately 58.08% of the total weight. This stage is associated with the thermal degradation of hemicellulose and cellulose, which decompose rapidly within this temperature interval. The DTG curve exhibits a pronounced peak at around 338 °C, indicating the maximum rate of mass loss and confirming cellulose decomposition as the dominant process. The third stage, referred to as secondary pyrolysis or slow carbonization, begins after 400 °C and proceeds gradually up to approximately 600–735 °C, resulting in an additional weight loss of about 36.49%. This stage is mainly attributed to the progressive decomposition of more thermally stable components and the formation of carbon-rich solid residues. The relatively steady mass-loss trend at higher temperatures indicates enhanced char stability, which is favorable for solid fuel or biochar applications.

Table 4 highlights the kinetic parameters obtained from the TGA data provide quantitative support for the multi-stage thermal decomposition behavior observed for CS. The primary pyrolysis stage, occurring in the temperature range associated with intensive mass loss (≈200–370 °C), is characterized by an apparent activation energy (Ea) of 122 kJ/mol, a pre-exponential factor (A) of 2.1×10^{13} min^{-1}, and a reaction order (n) of 1.1, with a high coefficient of determination (R^2 = 0.9738). These values indicate that this stage is kinetically well described by a near-first-order reaction model and is governed by the rapid thermal degradation of hemicellulose and cellulose, as identified in the TG/DTG curves.

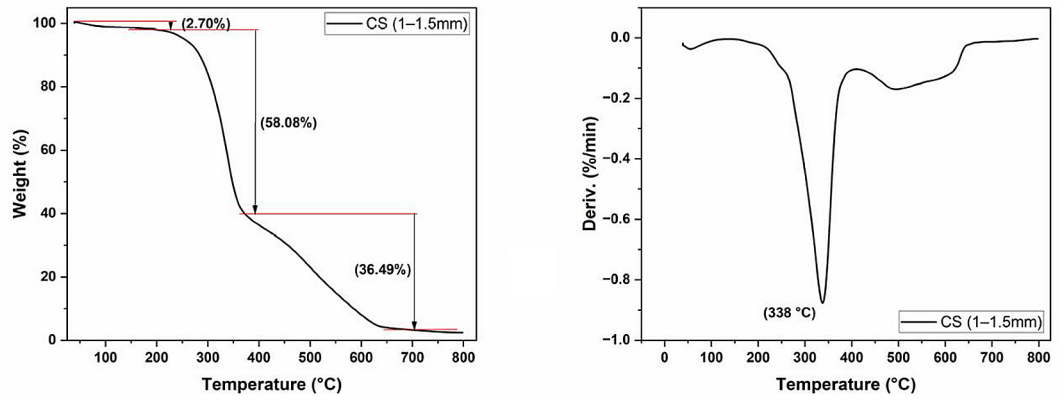

Figure 3. TGA (left) and DTG (right) graphs of CS sample (Elshareef et al., 2025)

Table 4. Kinetics parameters of CS pyrolysis

Stage	E_a (kJ/mol)	A (1/min)	n (-)	R^2 (-)
Primary pyrolysis	122	2.1E+13	1.1	0.9738
Secondary pyrolysis	53.8	5.22E+12	1.3	0.8163

In contrast, the secondary pyrolysis stage, corresponding to the high-temperature region above approximately 400 °C, exhibits a significantly lower activation energy of 53.8 kJ/mol, along with a pre-exponential factor of 5.22×10^{12} min^{-1} and a higher reaction order (n = 1.3), with a moderate fit quality ($R^2 = 0.8163$). This kinetic behavior aligns with the slow carbonization and char-forming processes observed in the later part of the TG curve, where mass loss proceeds gradually up to around 600–735 °C. The reduced activation energy indicates that secondary pyrolysis reactions, dominated by the decomposition of thermally stable structures and char rearrangement, are less energy-intensive than primary devolatilization. The higher reaction order suggests increased complexity of the reaction mechanism, likely involving overlapping reactions such as secondary cracking, aromatization, and structural reorganization of the carbon matrix.

FTIR analysis results of biomass samples

Figure 4a shows FTIR spectra of FW samples, showcasing the molecular functional groups in the raw biomass feedstock prior to HTC. The absorbance profiles reveal prominent peaks at approximately 3300–3400 cm^{-1} (broad O-H stretching from hydroxyl groups in carbohydrates and water), 2850–2950 cm^{-1} (C-H stretching in aliphatic chains from lipids and proteins), 1650 cm^{-1} (C=O stretching in amides or carboxylic acids), 1400–1450 cm^{-1} (C-H bending), and 1000–1100 cm^{-1} (C-O stretching in polysaccharides like cellulose and hemicellulose). These features confirm the organic-rich nature of FW, dominated by lignocellulosic and proteinaceous components. The high degree of spectral overlap across samples (e.g., 1FW-L, 2FW-L, 3FW-R, 4FW-C, and positional variants like left-corner, top, and bottom) indicates compositional homogeneity, which is advantageous for reproducible HTC yields. In the context of bio-coal production, the abundance of oxygen-containing groups highlights the potential for HTC to promote dehydration, decarboxylation, and aromatization, transforming the feedstock into energy-dense hydro-char with reduced O/C ratios and improved combustibility.

Figure 4b shows the FTIR spectra of CS samples, illustrating the functional group composition of the raw agricultural feedstock. Key absorption bands include a broad peak at 3200–3500 cm^{-1} (O-H stretching in lignocellulosic hydroxyls), 2800–3000 cm^{-1} (C-H stretching in methyl/methylene groups), 1600–1700 cm^{-1} (C=O stretching in hemicellulose and lignin), 1400–1500 cm^{-1} (aromatic C=C in lignin), and 1000–1200 cm^{-1} (C-O-C and C-O stretching in polysaccharides). These signatures underscore the lignocellulosic dominance in CS, with cellulose, hemicellulose, and lignin as primary components. The consistent spectral patterns across samples (1CS-C, 2CS-C, 3CS-LC, 4CS-RC) suggest minimal variability, ensuring reliable HTC processing. For bio-coal

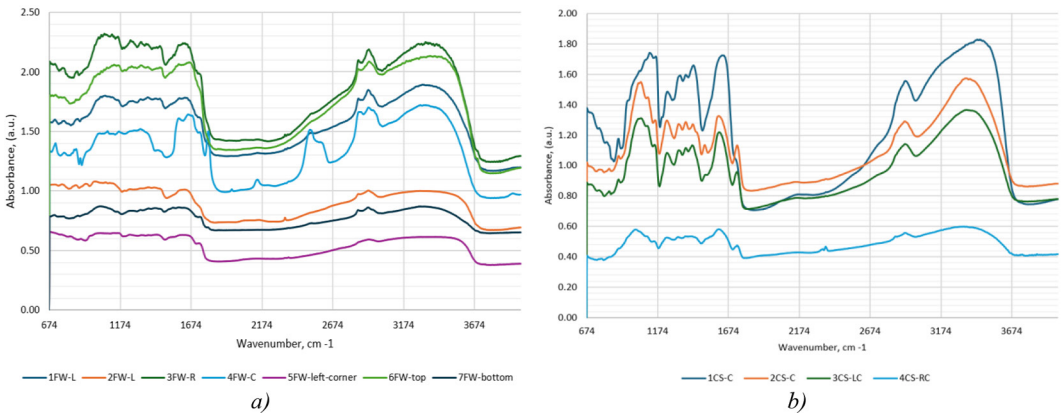

a) *b)*

Figure 4. FTIR results of FW (a) and CS (b) samples

production, the prevalence of oxygenated functionalities indicates HTC's efficacy in driving hydrolysis, dehydration, and polymerization reactions, yielding hydro-char with enhanced carbon content, lower volatility, and coal-like properties suitable for energy applications.

Comparison of FTIR spectra between FW and CS feedstocks

FTIR spectroscopy provides valuable insights into the functional group compositions of biomass feedstocks, which is crucial for optimizing HTC processes in bio-coal production. Comparing the FTIR spectra of FW and CS reveals both similarities and distinct differences reflective of their origins—FW as a heterogeneous municipal waste rich in organics from diverse sources, and CS as a lignocellulosic agricultural residue.

Key similarities include broad O-H stretching bands (3200–3500 cm^{-1} in CS; 3300–3400 cm^{-1} in FW), indicating hydroxyl groups from polysaccharides and moisture in both. Aliphatic C-H stretching (2800–3000 cm^{-1} in CS; 2850–2950 cm^{-1} in FW) and C-O/C-O-C stretching (1000–1200 cm^{-1} in CS; 1000–1100 cm^{-1} in FW) further highlight shared carbohydrate structures, such as cellulose and hemicellulose, making both suitable for HTC's dehydration and polymerization reactions.

However, notable differences underscore compositional variances: FW shows a prominent C=O peak at 1650 cm^{-1} (amides/carboxylic acids from proteins and lipids), absent or less intense in CS, which instead features stronger signals at 1600–1700 cm^{-1} (C=O in hemicellulose/lignin) and 1400–1500 cm^{-1} (aromatic C=C in lignin). FW's spectra also exhibit C-H bending at 1400–1450 cm^{-1}, suggesting more aliphatic content, while CS displays broader lignin-related aromatics. Spectral homogeneity is evident in both, with minimal variability across samples, but FW's profiles indicate higher oxygen-containing groups overall, potentially leading to greater hydro-char yield via enhanced decarboxylation during HTC.

In bio-coal contexts, FW's protein/lipid-derived functionalities may promote faster HTC kinetics and nitrogen-rich hydro-char for soil amendments, whereas CS's lignin dominance could yield more stable, carbon-dense bio-coal with coal-like aromaticity. Blending these feedstocks could balance these traits for optimized energy recovery and reduced ash issues.

CONCLUSIONS

The comprehensive characterization of MSW from Tashkent demonstrates that FW consistently constitutes the dominant fraction, with biodegradable organic matter (FW + bones + plant residues) exceeding 54 wt% across districts. This high organic load, rich in lignocellulosic constituents, underscores the suitability of urban FW as a primary feedstock for HTC aimed at bio-coal production.

Detailed compositional and thermal analyses further confirm the advantageous characteristics of FW for HTC processing. Structural carbohydrate profiling revealed a carbohydrate-dominant matrix with high cellulose and hemicellulose contents, complemented by significant lignin, aligning with biomass types that favor solid fuel pathways. Proximate and HHV measurements show that FW and CS can be used as a reliable feedstock for HTC which also can produce hydro-char competitive with sub-bituminous coal.

Spectroscopic and thermogravimetric analyses of FW and CS provide mechanistic insight into thermal behavior and chemical functionality relevant to HTC conversion. FTIR spectra highlight abundant oxygenated functional groups typical of lignocellulosic and proteinaceous matter, indicating strong potential for dehydration, decarboxylation, and aromatization reactions during HTC that drive carbon enrichment. TGA/DTG results delineate multistage decomposition — moisture loss, primary and secondary pyrolysis, and high-temperature degradation — with kinetics reflecting the degradation of hemicellulose, cellulose, and lignin fractions, consistent with established biomass pyrolysis models (e.g., primary and secondary activation energies differ significantly). Collectively, these findings validate FW and CS as a homogenous, high-energy HTC feedstocks capable of producing hydro-char with coal-like properties, and they support strategic integration of urban organic waste streams into sustainable bio-energy frameworks.

This study contributes to future researches on conversion of organic wastes by HTC technology, which advances the SDG goals of: Affordable and Clean Energy, Sustainable Cities and Communities, and Responsible Consumption.

Acknowledgements

The team appreciates the support from the College of Mechanical and Electrical Engineering of the Shihezi University (Xinjiang, China),

and Bioenergy and Environment Science & Technology Laboratory, College of Engineering, China Agricultural University (Beijing, China).

REFERENCES

1. Antero, R. V. P., Alves, A. C. F., De Oliveira, S. B., Ojala, S. A., Brum, S. S. (2020). Challenges and alternatives for the adequacy of hydrothermal carbonization of lignocellulosic biomass in cleaner production systems: A review. *Journal of Cleaner Production*, *252*, 119899. https://doi.org/10.1016/j.jclepro.2019.119899
2. ASTM, I. (2016). *Standard test method for determination of the composition of unprocessed municipal solid waste* (D5231-92). https://doi.org/10.1520/D5231-92R16
3. Babinszki, B., Jakab, E., Sebestyén, Z., Blazsó, M., Berényi, B., Kumar, J., Krishna, B. B., Bhaskar, T., Czégény, Z. (2020). Comparison of hydrothermal carbonization and torrefaction of azolla biomass: Analysis of the solid products. *Journal of Analytical and Applied Pyrolysis*, *149*, 104844. https://doi.org/10.1016/j.jaap.2020.104844
4. Borges, A.D.S., Cardoso, M. Oliveira, M. (2026). Thermochemical evaluation of biochars properties from Portuguese agro-forestry residues for solid fuel applications. *Sci Rep 16*, 1120. https://doi.org/10.1038/s41598-025-30809-5
5. Elkhalifa, S., Parthasarathy, P., Mackey, H. R., Al-Ansari, T., Elhassan, O., Mansour, S., McKay, G. (2025). Biochar development from thermal TGA studies of individual food waste vegetables and their blended systems. *Biomass Conversion and Biorefinery*, *15*(23), 29965–29982. https://doi.org/10.1007/s13399-022-02441-0
6. Elshareef, H., Tursunov, O., Ren, S., Śpiewak, K., Mohamed, A. R., Fu, Y., Dong, R., Zhou, Y. (2025). Investigation of bio-oil and biochar derived from cotton stalk pyrolysis: Effect of different reaction conditions. *Resources*, *14*(5), 75. https://doi.org/10.3390/resources14050075
7. Fu, M.-M., Mo, C.-H., Li, H., Zhang, Y.-N., Huang, W.-X., Wong, M. H. (2019). Comparison of physicochemical properties of biochars and hydrochars produced from food wastes. *Journal of Cleaner Production*, *236*, 117637. https://doi.org/10.1016/j.jclepro.2019.117637
8. Ganeshan, G., Shadangi, K. P., Mohanty, K. (2018). Degradation kinetic study of pyrolysis and co-pyrolysis of biomass with polyethylene terephthalate (PET) using Coats–Redfern method. *Journal of Thermal Analysis and Calorimetry*, *131*(2), 1803–1816. https://doi.org/10.1007/s10973-017-6597-5
9. Gao, L., Volpe, M., Lucian, M., Fiori, L., Goldfarb, J. L. (2019). Does hydrothermal carbonization as a biomass pretreatment reduce fuel segregation of coal-biomass blends during oxidation? *Energy Conversion and Management*, *181*, 93–104. https://doi.org/10.1016/j.enconman.2018.12.009
10. Indira, V., Parameswaran, G. (1986). Thermal decomposition kinetics of salicylideneaminofluorene complexes of cobalt(II) and nickel(II). *Thermochimica Acta*, *101*, 145–154. https://doi.org/10.1016/0040-6031(86)80049-1
11. Kang, K., Nanda, S., Sun, G., Qiu, L., Gu, Y., Zhang, T., Zhu, M., Sun, R. (2019). Microwave-assisted hydrothermal carbonization of corn stalk for solid biofuel production: Optimization of process parameters and characterization of hydrochar. *Energy*, *186*, 115795. https://doi.org/10.1016/j.energy.2019.07.125
12. Khan, T. A., Saud, A. S., Jamari, S. S., Rahim, M. H. A., Park, J.-W., Kim, H.-J. (2019). Hydrothermal carbonization of lignocellulosic biomass for carbon rich material preparation: A review. *Biomass and Bioenergy*, *130*, 105384. https://doi.org/10.1016/j.biombioe.2019.105384
13. Krysanova, K., Krylova, A., Zaichenko, V. (2019). Properties of biochar obtained by hydrothermal carbonization and torrefaction of peat. *Fuel*, *256*, 115929. https://doi.org/10.1016/j.fuel.2019.115929
14. Liu, J., Huang, S., Chen, K., Wang, T., Mei, M., Li, J. (2020). Preparation of biochar from food waste digestate: Pyrolysis behavior and product properties. *Bioresource Technology*, *302*, 122841. https://doi.org/10.1016/j.biortech.2020.122841
15. Mazumder, S., Saha, P., Reza, M. T. (2022). Co-hydrothermal carbonization of coal waste and food waste: Fuel characteristics. *Biomass Conversion and Biorefinery*, *12*(1), 3–13. https://doi.org/10.1007/s13399-020-00771-5
16. Özsin, G., Pütün, A. E. (2017). Kinetics and evolved gas analysis for pyrolysis of food processing wastes using TGA/MS/FT-IR. *Waste Management*, *64*, 315–326. https://doi.org/10.1016/j.wasman.2017.03.020
17. Pecchi, M., Patuzzi, F., Benedetti, V., Di Maggio, R., Baratieri, M. (2020). Kinetic analysis of hydrothermal carbonization using high-pressure differential scanning calorimetry applied to biomass. *Applied Energy*, *265*, 114810. https://doi.org/10.1016/j.apenergy.2020.114810
18. Periyavaram, S. R., K, B., Uppala, L., Reddy, P. H. P. (2023). Hydrothermal carbonization of food waste: Process parameters optimization and biomethane potential evaluation of process water. *Journal of Environmental Management*, *347*, 119132. https://doi.org/10.1016/j.jenvman.2023.119132
19. Reza, M. T., Andert, J., Wirth, B., Busch, D., Pielert, J., Lynam, J. G., Mumme, J. (2014). Hydrothermal carbonization of biomass for energy and crop production. *Applied Bioenergy*, *1*(1). https://doi.org/10.2478/apbi-2014-0001

20. Saba, A., Saha, P., Reza, M. T. (2017). Co-hydrothermal carbonization of coal-biomass blend: Influence of temperature on solid fuel properties. *Fuel Processing Technology*, *167*, 711–720. https://doi.org/10.1016/j.fuproc.2017.08.016
21. Sharma, H. B., Sarmah, A. K., Dubey, B. (2020). Hydrothermal carbonization of renewable waste biomass for solid biofuel production: A discussion on process mechanism, the influence of process parameters, environmental performance and fuel properties of hydrochar. *Renewable and Sustainable Energy Reviews*, *123*, 109761. https://doi.org/10.1016/j.rser.2020.109761
22. Tursunov, O., Karimov, I., Abduganiyev, N., Kodirov, D., Yuhnevich, G., Md. Ali, U. F., Mohamed, A. R., Duong, V.-H., Nurfahasdi, M., Abdivakhidov, K. (2025). Characterisation and gas chromatography–mass spectrometry analysis of products from pyrolysis of municipal solid waste using a fixed-bed reactor. *Journal of Ecological Engineering*, *26*(7), 157–170. https://doi.org/10.12911/22998993/203363
23. Tursunov, O., Karimov, I., Śpiewak, K., Hu, X., Zhou, Y., Kustov, A., Ali, U. F. M., Uvarov, R. (2024). Comprehensive study on social, compositional and thermal aspects of household solid waste for waste-to-energy potential estimation in Tashkent city. *Energy Reports*, *12*, 430–441. https://doi.org/10.1016/j.egyr.2024.06.035
24. Tursunov, O., Śpiewak, K., Abduganiev, N., Yang, Y., Kustov, A., Karimov, I. (2023). Thermogravimetric and thermovolumetric study of municipal solid waste (MSW) and wood biomass for hydrogen-rich gas production: A case study of Tashkent region. *Environmental Science and Pollution Research*, *30*(52), 112631–112643. https://doi.org/10.1007/s11356-023-30368-0
25. Wang, T., Si, B., Gong, Z., Zhai, Y., Cao, M., Peng, C. (2020). Co-hydrothermal carbonization of food waste-woody sawdust blend: Interaction effects on the hydrochar properties and nutrients characteristics. *Bioresource Technology*, *316*, 123900. https://doi.org/10.1016/j.biortech.2020.123900
26. Wilk, M., Śliz, M., Gajek, M. (2021). The effects of hydrothermal carbonization operating parameters on high-value hydrochar derived from beet pulp. *Renewable Energy*, *177*, 216–228. https://doi.org/10.1016/j.renene.2021.05.112
27. Wu, S., Wang, Q., Cui, D., Wang, X., Wu, D., Bai, J., Xu, F., Wang, Z., Zhang, J. (2023). Analysis of fuel properties of hydrochar derived from food waste and biomass: Evaluating varied mixing techniques pre/post-hydrothermal carbonization. *Journal of Cleaner Production*, *430*, 139660. https://doi.org/10.1016/j.jclepro.2023.139660
28. Wüst, D., Rodriguez Correa, C., Suwelack, K. U., Köhler, H., Kruse, A. (2019). Hydrothermal carbonization of dry toilet residues as an added-value strategy – Investigation of process parameters. *Journal of Environmental Management*, *234*, 537–545. https://doi.org/10.1016/j.jenvman.2019.01.005
29. Xu, J., Zhang, J., Huang, J., He, W., Li, G. (2020). Conversion of phoenix tree leaves into hydro-char by microwave-assisted hydrothermal carbonization. *Bioresource Technology Reports*, *9*, 100353. https://doi.org/10.1016/j.biteb.2019.100353
30. Xu, Y., Chen, B. (2013). Investigation of thermodynamic parameters in the pyrolysis conversion of biomass and manure to biochars using thermogravimetric analysis. *Bioresource Technology*, *146*, 485–493. https://doi.org/10.1016/j.biortech.2013.07.086
31. Yan, M., Chen, F., Li, T., Zhong, L., Feng, H., Xu, Z., Hantoko, D., Wibowo, H. (2023). Hydrothermal carbonization of food waste digestate solids: Effect of temperature and time on products characteristic and environmental evaluation. *Process Safety and Environmental Protection*, *178*, 296–308. https://doi.org/10.1016/j.psep.2023.08.010
32. Yusuf, I., Flagiello, F., Ward, N. I., Arellano-García, H., Avignone-Rossa, C., Felipe-Sotelo, M. (2020). ;Valorisation of banana peels by hydrothermal carbonisation: Potential use of the hydrochar and liquid by-product for water purification and energy conversion. *Bioresource Technology Reports*, *12*, 100582. https://doi.org/10.1016/j.biteb.2020.100582
33. Zhou, L., Wang, Y., Huang, Q., Cai, J. (2006). Thermogravimetric characteristics and kinetic of plastic and biomass blends co-pyrolysis. *Fuel Processing Technology*, *87*(11), 963–969. https://doi.org/10.1016/j.fuproc.2006.07.002